Observationally constrained analysis of sulfur cycle in the marine atmosphere with NASA ATom measurements and AeroCom model simulations

Huisheng Bian[1,2], Mian Chin[2], Peter Colarco[2], Eric C. Apel[3], Donald R. Blake[4], Karl Froyd[5], Rebecca S. Hornbrook[3], Jose Jimenez[6,5], Pedro Campuzano Jost[6,5], Michael Lawler[5,7], Mingxu Liu[8], Marianne Tronstad Lund[9], Hitoshi Matsui[8], Benjamin A. Nault[6,5,10,11], Joyce E. Penner[12], Andrew W. Rollins[5,13], Gregory Schill[7], Ragnhild B. Skeie[9], Hailong Wang[14], Lu Xu[15,16], Kai Zhang[14], and Jialei Zhu[17]

[1]Goddard Earth Sciences Technology and Research (GESTAR) II, University of Maryland at Baltimore County, Baltimore, MD, USA.
[2]NASA Goddard Space Flight Center, Greenbelt, MD, USA.
[3]Atmospheric Chemistry Observations & Modeling Laboratory, National Center for Atmospheric Research, Boulder, CO, USA,
[4]Department of Chemistry, University of California Irvine, CA, USA.
[5]Cooperative Institute for Research in Environmental Sciences, University of Colorado, Boulder, CO, USA.
[6]Department of Chemistry, University of Colorado, Boulder, CO, USA.
[7]NOAA Chemical Sciences Laboratory, Boulder, CO, USA.
[8]Graduate School of Environmental Studies, Nagoya University, Nagoya, Japan.
[9]CICERO Center for International Climate Research, Oslo, Norway.
[10]Now at: Department of Environmental Health and Engineering, Whiting School of Engineering, The Johns Hopkins, Baltimore, MD, USA
[11]Now at: Center for Aerosol and Cloud Chemistry, Aerodyne Research, Inc., Billerica, MA, USA
[12]Dept. of Atmospheric, Oceanic and Space Sciences, University of Michigan, Ann Arbor, Michigan, USA.
[13]NOAA Earth System Research Laboratory, Chemical Sciences Division, Boulder, CO, USA.
[14]Atmospheric Sciences and Global Change Division, Pacific Northwest National Laboratory, Richland, WA, USA.
[15]Division of Geological and Planetary Sciences, California Institute of Technology, Pasadena, CA, USA.
[16]Department of Energy, Environmental and Chemical Engineering, Washington University in St. Louis, Missouri, USA.
[17]Institute of Surface-Earth System Science, School of Earth System Science, Tianjin University, Tianjin, China.

Correspondence to: Huisheng Bian (huisheng.bian@nasa.gov)

Supplementary Material

We further analyze observations and simulations, similar to Figs 2–4, but include all measurements of SO_4, SO_2, and DMS in Figs S1–3, respectively. Specifically, the negative values measured by AMS, CIMS, and LIF and the LDL value "-888" measured by TOGA and WAS were included, and the value "-888" was replaced with "0". Of course, the observed median and mean values dropped substantially, by 17% and 13% for SO_4, and by 34% and 34% for SO_2. DMS is unique in that most of its measurements are reported as "-888", which results in a median of zero in Fig. S3 and a 86% drop in the mean. However, the model statistics vary relatively small, 4% and 13% for SO_4 and 12% and 15% for SO_2. The median modeled DMS decreased from 56.6 pptv to 0.7 pptv and a mean decrease of 76%.

The observed and simulated vertical profiles in each ATom are further shown in Figs. S4-7 to reveal details of seasonal changes. For example, the SO_2 values measured by LIF in Fig. 6 are lower than the average SO_2 values measured by CIMS, but the two SO_2 profiles shown in Fig. S5 in ATom-4 are in good agreement when the LIF was onboard. This means that the SO_2 measured by CIMS during ATom-1 to -3 is higher than the SO_2 measured during ATom-4. A discussion of some seasonal characteristics has been given in main text Sect. 3.2.

Overall model performance has been demonstrated in Figs 9-11. The performance of each model on a regional and seasonal basis is further provided in Figs S8-10 to help modelers identify strengths and weaknesses of the model's sulfur simulations. Also, the mean values shown in the figures add information about extreme pollution.

As we mentioned in the main text, pollution levels in the model world and the observed world can differ substantially in certain regions of each ATom, and this difference can be caused by the majority of models or a few individual models. Each model performs better or worse than the others at every time and place. For example, in summer and winter, the CAM-ATRAS model gave the highest estimates of atmospheric SO_4 in the oceanic boundary layer (BL), but the IMPACT and OsloCTM3 models gave the highest estimates of atmospheric SO_4 in the free troposphere (Fig. S8). All models except the GEOS model generally overestimate SO_4 in the atmosphere. On the other hand, the E3SM model gives significantly higher SO_2 compared with the measurements and other models in BL (Fig. S9). Unlike the case of SO_4, all models tend to underestimate SO_2 in the free troposphere, with some exceptions such as the GEOS model in the North Pacific mid-high-latitude winter (ATom-2) and the CAM-ATRAS and IMAPCT models in the South Atlantic mid-latitude autumn (ATom-4). The overestimation of the DMS multi-model median in Fig. S10 is clearly attributable to the contribution of all models, with the models CAM-ATRAS and OsloCTM3 being more prominent.

The mean values of SO_4, SO_2, and DMS are generally higher than the median values at most times and locations, and the ratio of mean-to-median value in the BL is even greater than that in the free troposphere. Sometimes the ratio is very high (e.g., > 10), which means that extreme contamination has been identified.

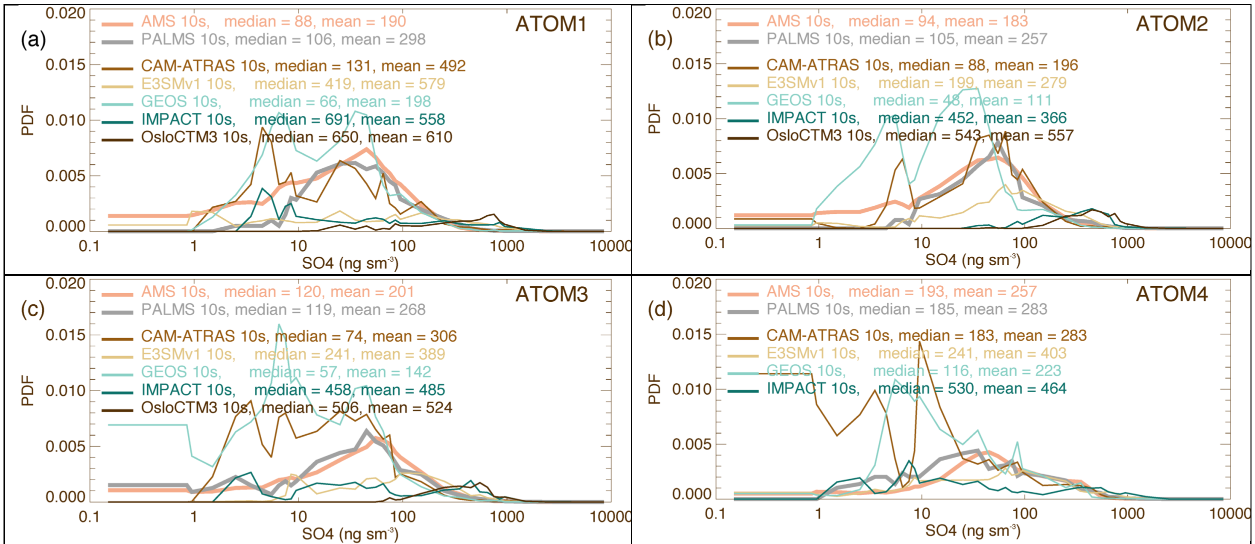

Figure S1. Similar to Fig. 2 but the median/mean values are calculated as long as the measurements are available even the values are negative.

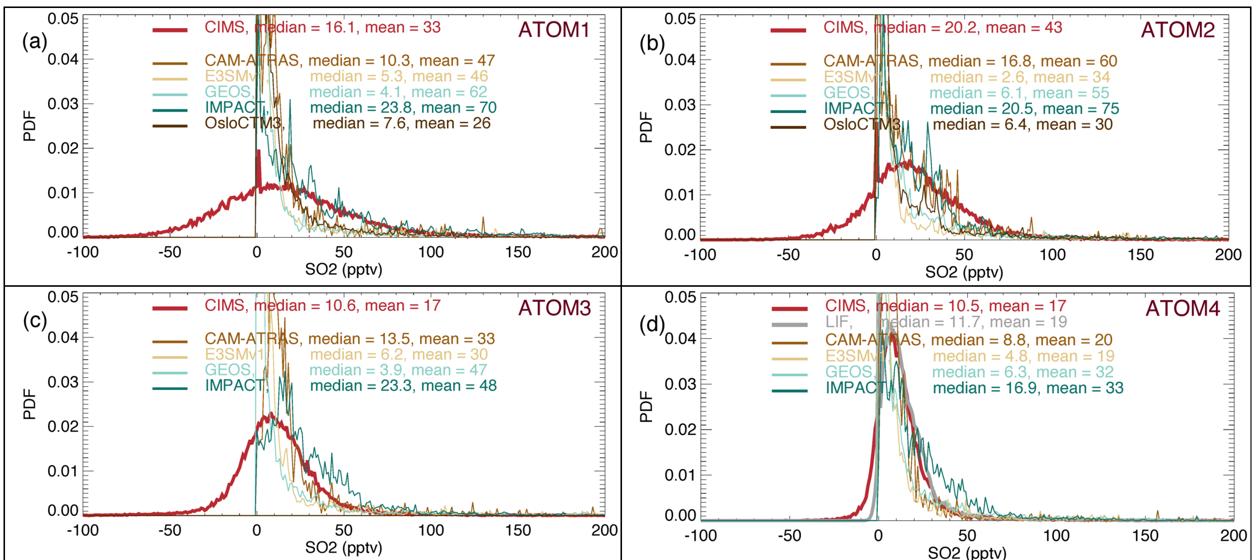

Figure S2. Similar to Fig. 3, but the median/mean values are calculated as long as the measurements are available even the values are negative.

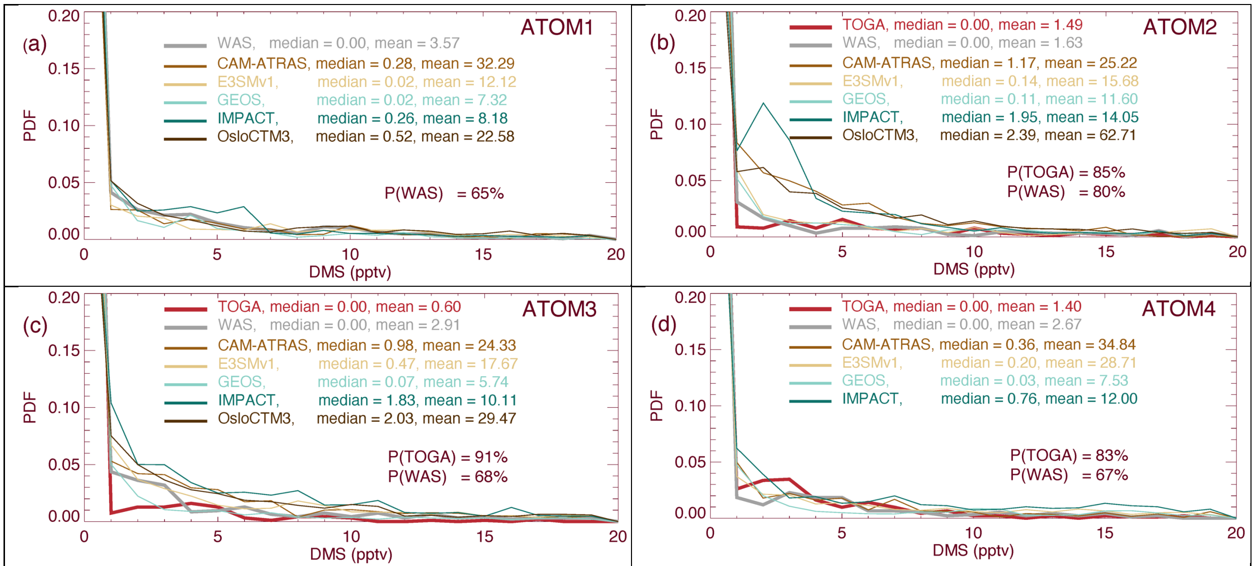

Figure S3. Similar to Fig. 4, but instead of excluding the "-888" measurements, these are replaced with 0 as suggested by the instrument PIs. The percentage (P) of the measured "-888" is given for TOGA and WAS measurement data. Model median/mean values are calculated when measurements including these "-888" are available.

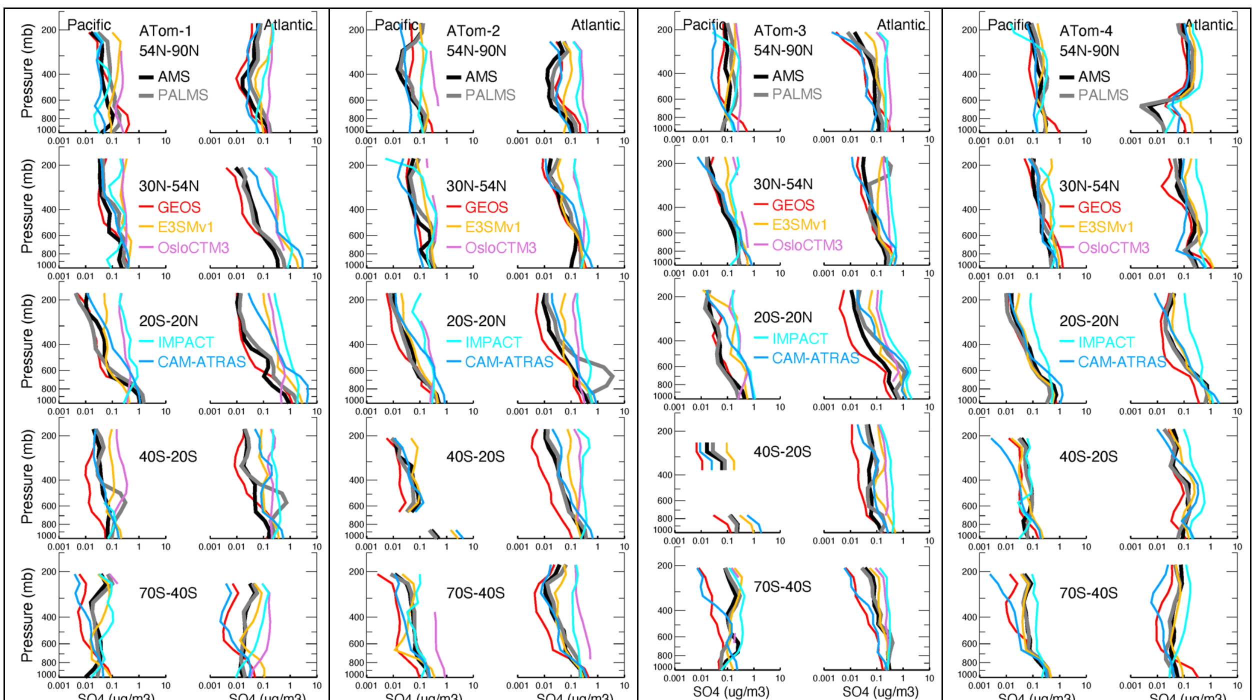

Figure S4. Observed and modeled vertical profiles of SO_4 in 1-km vertical bins for four ATom deployments shown from left to right. ATom measurements are shown in black and grey lines while model results are shown in color lines. Comparisons are conducted only when both observational measurements above detect limitation are available. Comparisons are separated into five latitude bands from the northern to the southern hemisphere, and into Pacific and Atlantic Basins.

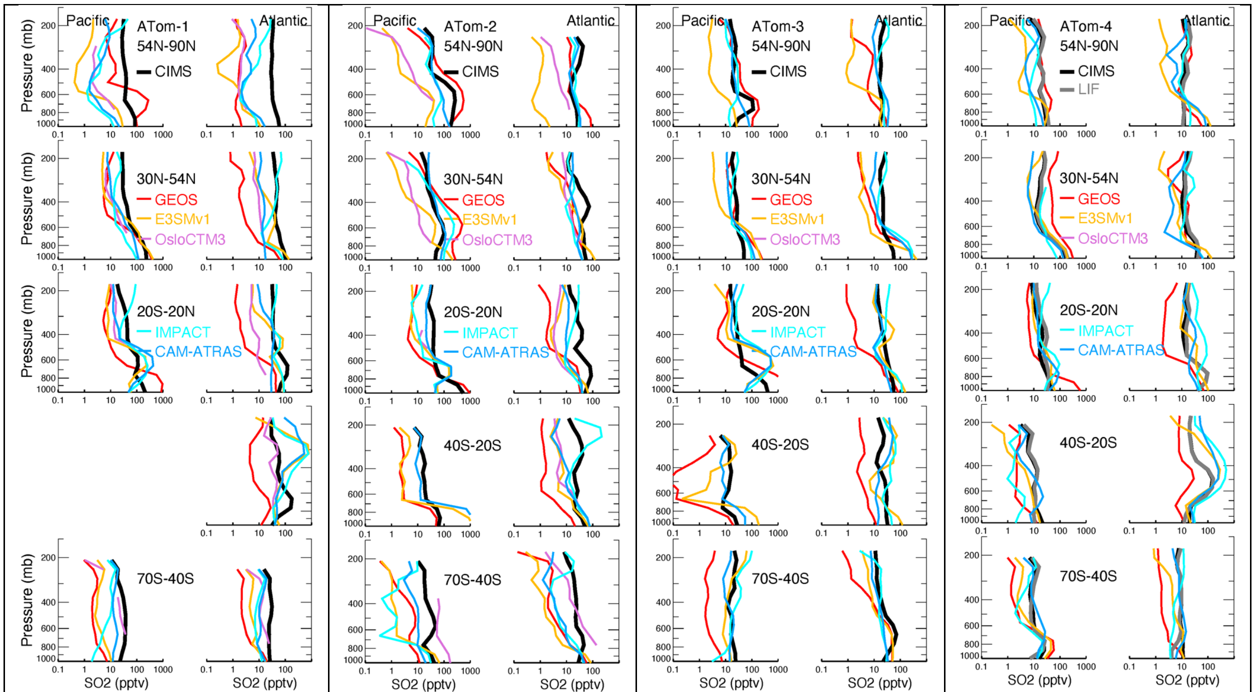

Figure S5. Similar to Fig. S4 but for SO_2.

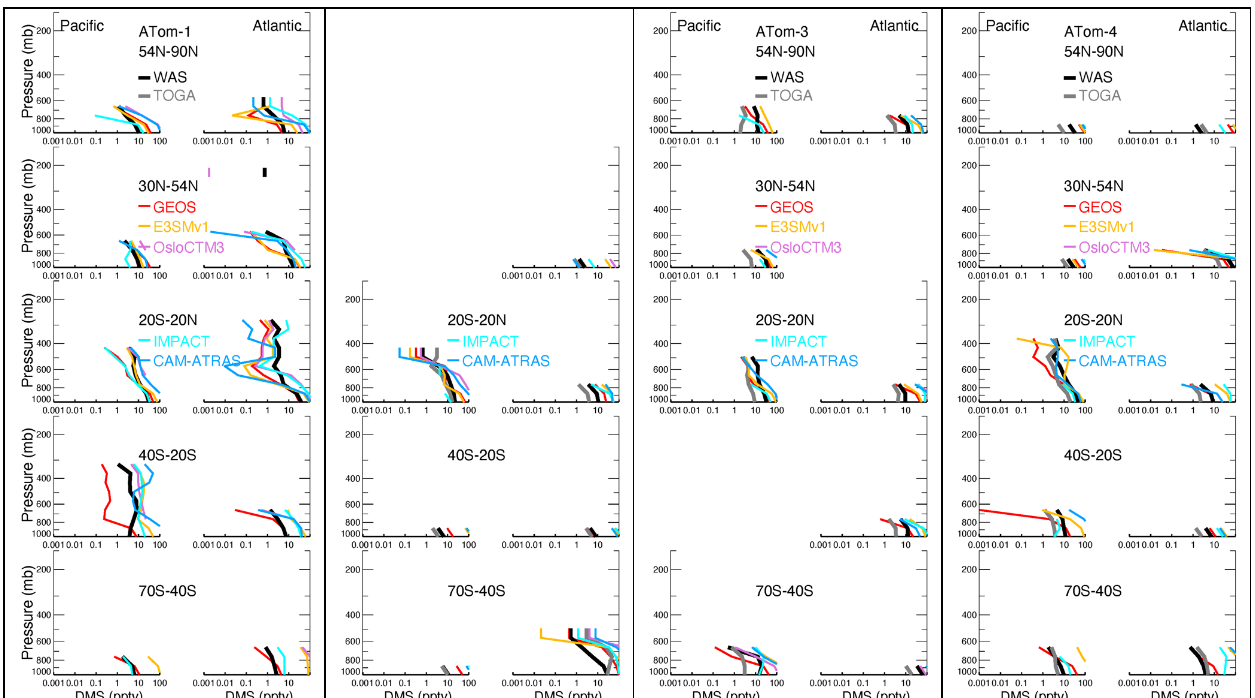

Figure S6. Similar to Fig. S4 but for DMS.

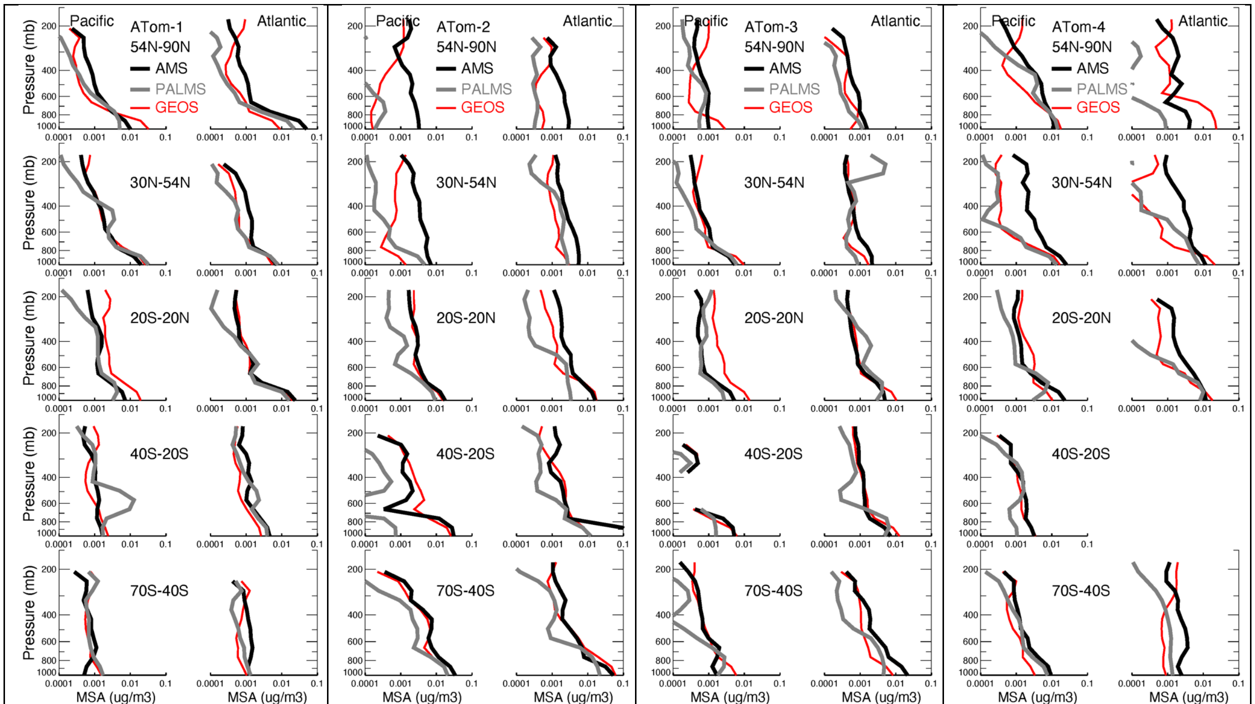

Figure S7. Similar to Fig. S4 but for MSA.

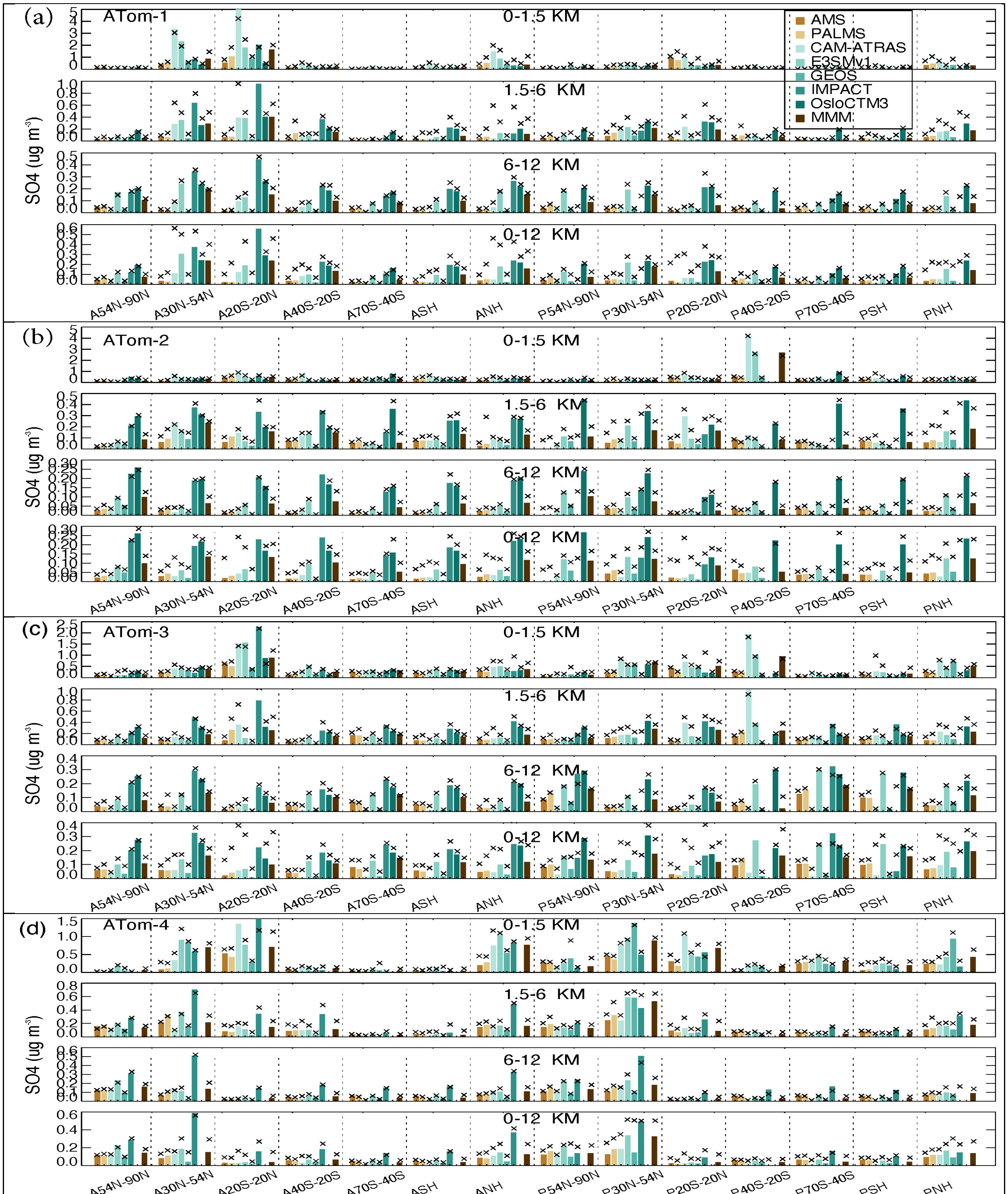

Figure S8. Median (histogram) and mean (symbol x) values of SO_4 from two measurements (red and yellow), five model simulations (other bluish colors), and multi-model simulation (black) analyzed over five latitudinal bands and SH and NH over Atlantic and Pacific oceans in four vertical layers (i.e., 0-1.5 km, 1.5-6 km, 6-12km, and 0-12 km) for four ATom deployments (a-d).

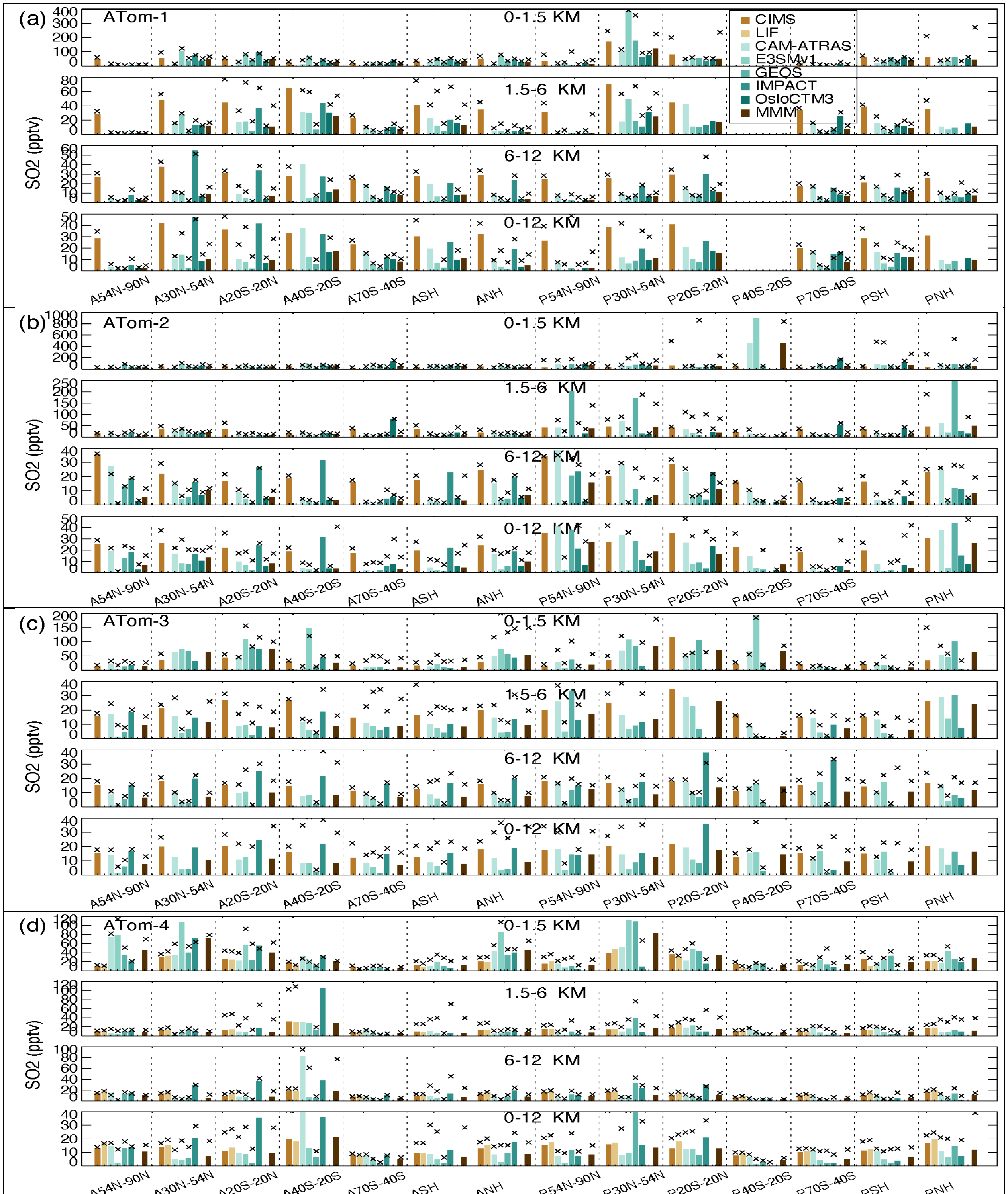

Figure S9. Similar to Fig. S8 but for SO_2.

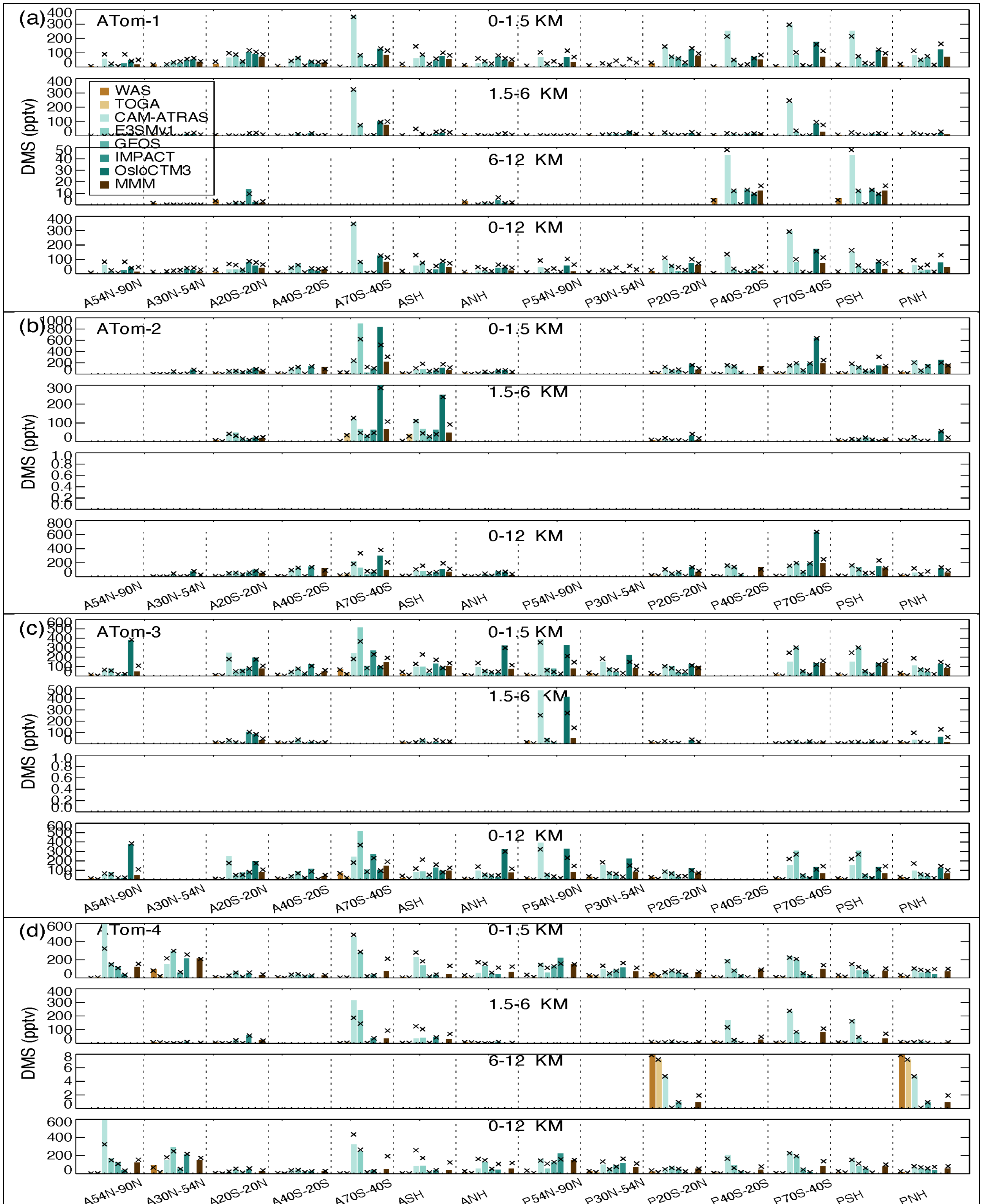

Figure S10. Similar to Fig. S8 but for DMS.